

Supplementary material

EDL structure of ionic liquid-MXene-based supercapacitor and hydrogen bond role on the interface: A molecular dynamics simulation investigation

Ziyi Wang ^a, Junwu Chen ^b, Yao Li ^b, Kun Dong ^{*b} and Yinghao Yu^{*a}

^a School of Chemistry and Chemical Engineering, South China University of Technology, Guangzhou, Guangdong 510641, P.R China.

^b Beijing Key Laboratory of Ionic Liquids Clean Process, State Key Laboratory of Multiphase Complex Systems, Institute of Process Engineering, Chinese Academy of Sciences, Beijing 100190, P.R. China

Corresponding authors: dongkun@ipe.ac.cn; ceyhyu@scut.edu.cn

Table S1 Lennard-Jones components and point charge parameters for $\text{Ti}_3\text{C}_2\text{O}_2$.

Atom	L-J parameters and point charge		
	$\epsilon/\text{kcal.mol}^{-1}$	$\sigma/\text{\AA}$	charge/ e^-
Ti-inner	0.6087	1.9565	0.68
Ti-outer	0.6087	1.9565	1.04
C	0.0660	3.5000	-0.74
O	0.1554	3.1656	-0.64

Table S2 Lennard-Jones components and point charge parameters for $\text{Ti}_3\text{C}_2(\text{OH})_2$.

Atom	Lennard-Jones and point charge parameters		
	$\epsilon/\text{kcal.mol}^{-1}$	$\sigma/\text{\AA}$	charge/ e^-
Ti-inner	0.6087	1.9565	0.64
Ti-outer	0.6087	1.9565	0.88
C	0.0660	3.5000	-0.76
O	0.1554	3.1656	-0.79
H	0.1554	1.5000	0.35

Table S3 The ion diffusion coefficients ($10^{-6} \text{ cm}^2 \text{ s}^{-1}$) of the ILs ($[\text{HEMIm}][\text{NTf}_2]$ and $[\text{EMIM}][\text{NTf}_2]$) in the bulk

	D_{cation}	D_{anion}	$D_{\text{cation}} + D_{\text{anion}}$
$[\text{EMIM}][\text{NTf}_2]$	2.27	1.94	4.21
$[\text{HEMIm}][\text{NTf}_2]$	1.77	1.41	3.18

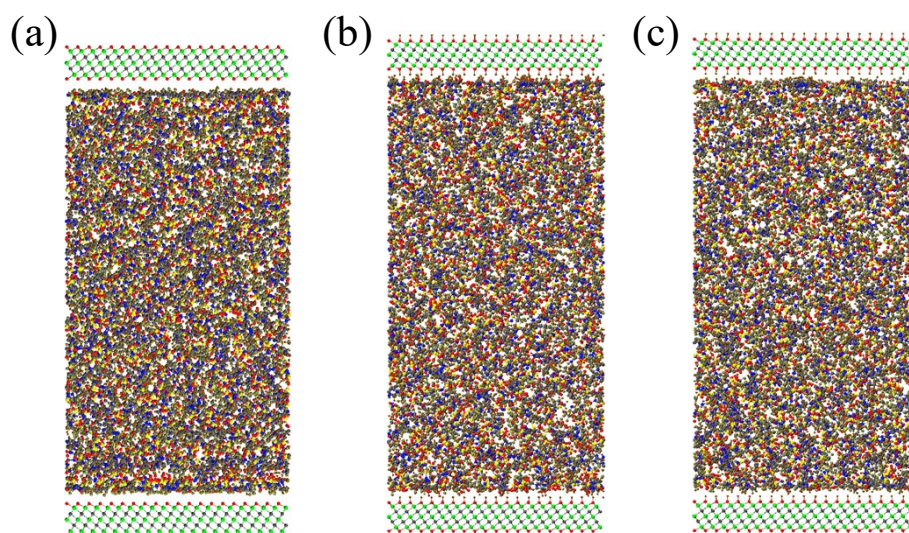


Fig. S1 A snapshot of the simulation box composed of (a) the [EMIM][NTf₂] and Ti₃C₂O₂, (b) the [HEMIm][NTf₂] and Ti₃C₂(OH)₂, (c) the [EMIM][NTf₂] and Ti₃C₂(OH)₂

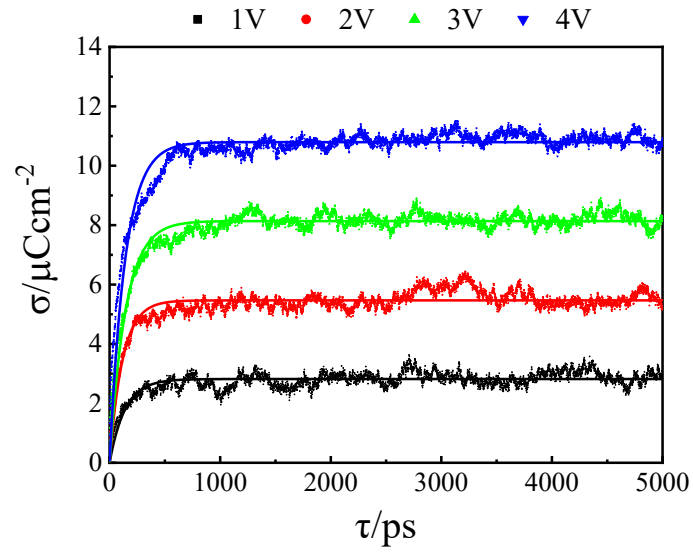


Fig. S2 Evolution of the charge density σ on electrode surface during the charging process with applying a series of potential differences to the $\text{Ti}_3\text{C}_2\text{O}_2$ electrodes for $[\text{HEMIm}][\text{NTf}_2]$.

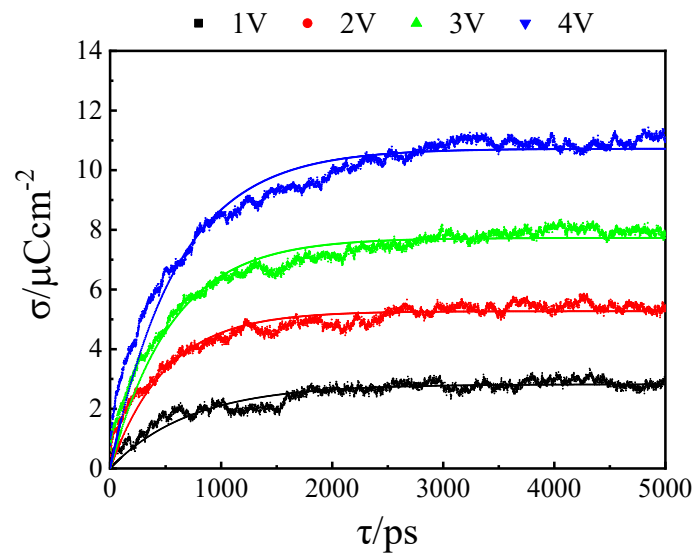


Fig. S3 Evolution of the charge density σ on electrode surface during the charging process with applying a series of potential differences to the $\text{Ti}_3\text{C}_2\text{O}_2$ electrodes for [EMIM] $[\text{NTf}_2]$.

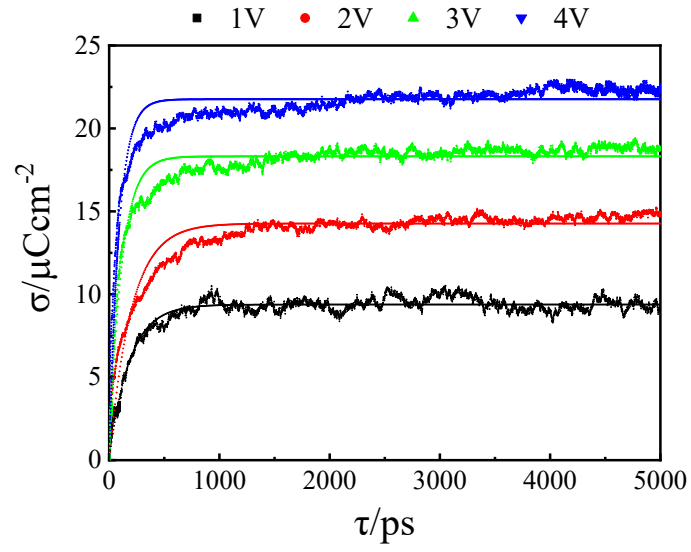


Fig. S4 Evolution of the charge density σ on electrode surface during the charging process with applying a series of potential differences to the $\text{Ti}_3\text{C}_2(\text{OH})_2$ electrodes for $[\text{HEMIm}][\text{NTf}_2]$.

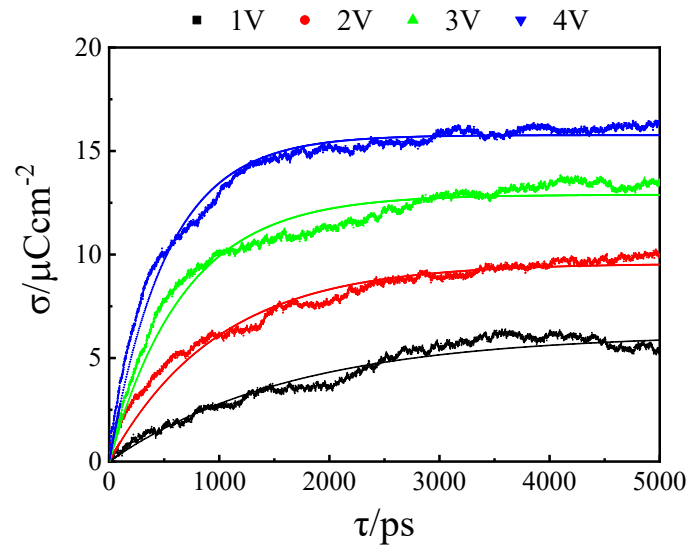


Fig. S5 Evolution of the charge density σ on electrode surface during the charging process with applying a series of potential differences to the $\text{Ti}_3\text{C}_2(\text{OH})_2$ electrodes for [EMIM] $[\text{NTf}_2]$.

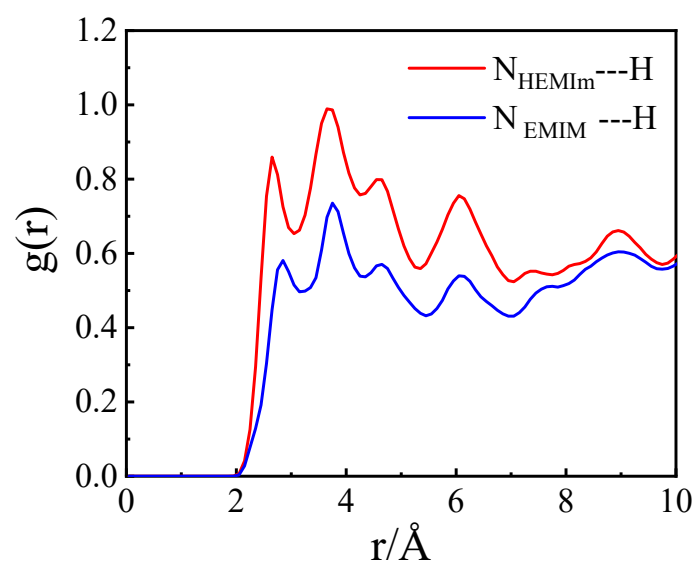


Fig. S6 Radial distribution function between N atoms in cations and H atoms in the $\text{Ti}_3\text{C}_2(\text{OH})_2$ electrodes at PZC.

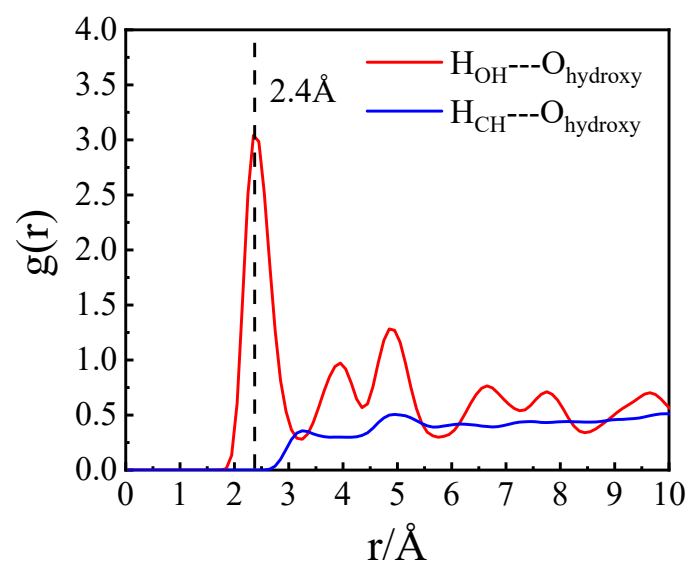


Fig. S7 Radial distribution function between H atoms of cations and O atoms of the $\text{Ti}_3\text{C}_2(\text{OH})_2$ electrodes at PZC.

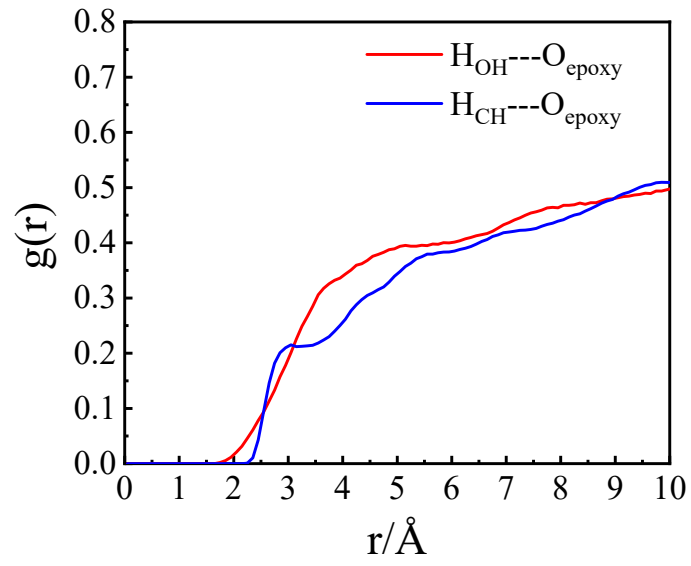


Fig. S8 Radial distribution function between H atoms of cations and O atoms of the $\text{Ti}_3\text{C}_2\text{O}_2$ electrodes at PZC.

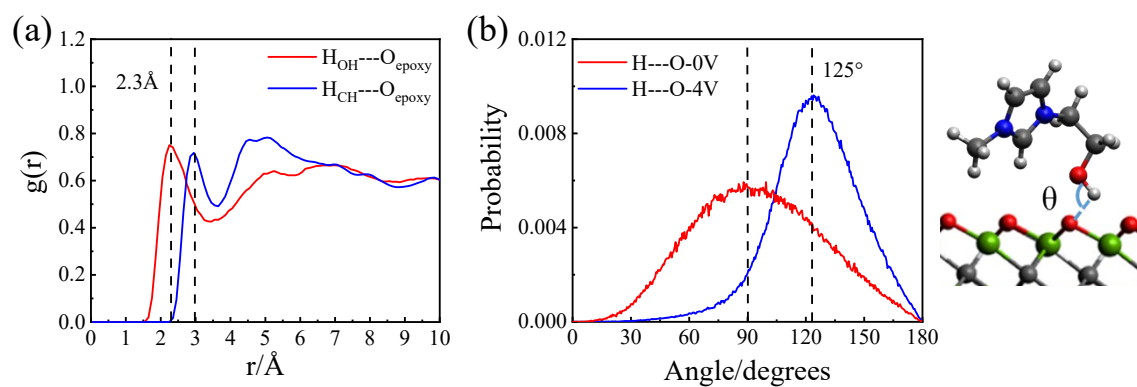
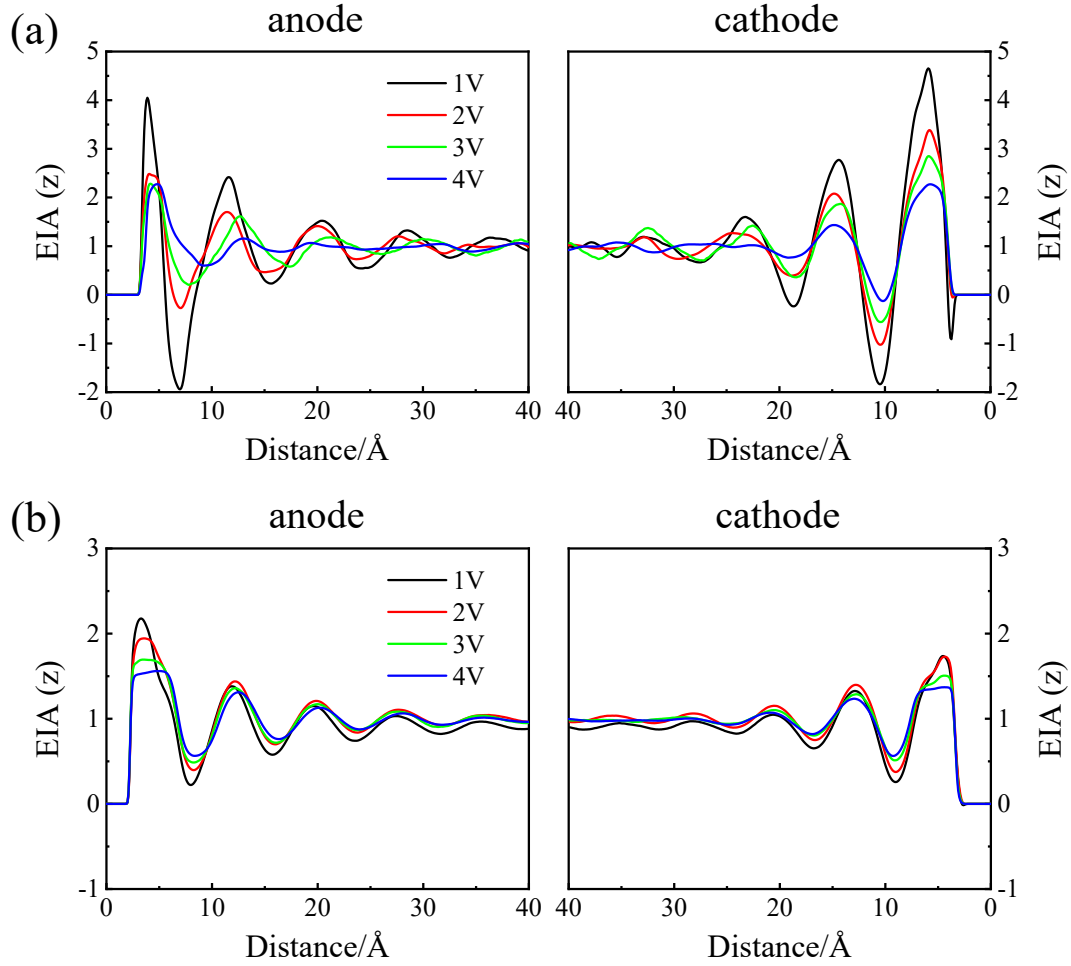


Fig. S9 (a) Radial distribution function between H atoms of cations and O atoms of $\text{Ti}_3\text{C}_2\text{O}_2$ electrodes at $\Delta\Psi = 4\text{V}$. The oxygen atoms in termination of the $\text{Ti}_3\text{C}_2\text{O}_2$ electrodes are denoted by O_{epoxy} . (b) distribution of the O-H...O angle between H_{OH} and O_{epoxy} within the distance less than 3 \AA at $\Delta\Psi = 0$ and 4V.

We quoted the calculation method of effective ion accumulation factor (EIA) to evaluate the degree of screening efficiency, following Feng

$$EIA(z) = \frac{\int_0^z [\rho_{N,\alpha}(s) - \rho_{N,\alpha}^{\cdot}(s)] ds}{|\sigma|/e}$$

where z is the distance from the electrode surface, σ is the absolute value of the charge in the electrode, e is the electron charge, and $\rho_{counter-ion}$ and ρ_{co-ion} are the number density of the counterion and coion, respectively.



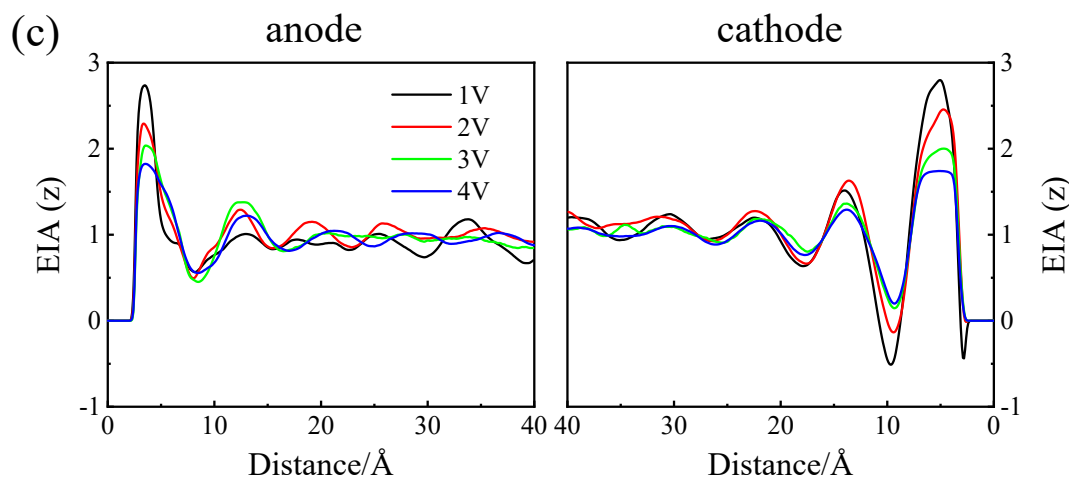


Fig. S10 EIA factor as a function of distance from the MXene electrode with different applied potentials. EIA profile for [EMIM][TFSI] at $\text{Ti}_3\text{C}_2\text{O}_2$ electrode and $\text{Ti}_3\text{C}_2(\text{OH})_2$ electrode (a, c) and for [HEMIm][NTf₂] at $\text{Ti}_3\text{C}_2(\text{OH})_2$ electrode (b).

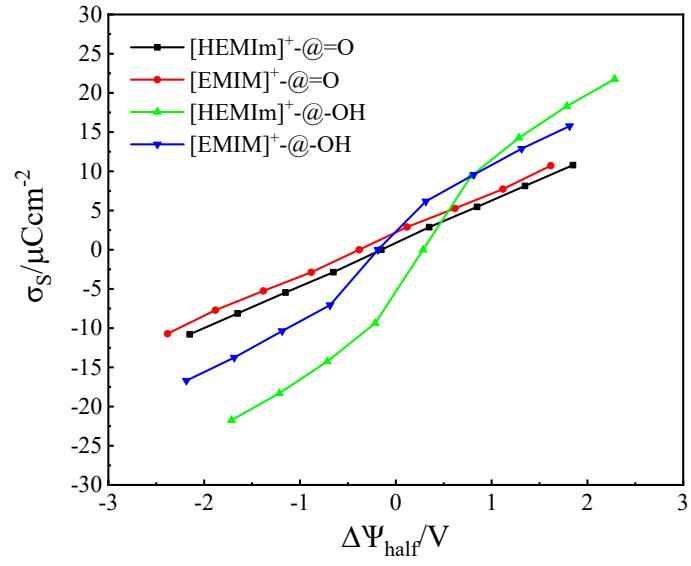


Fig. S11 Surface charge σ_s as a function of the half potential drop across the interface (

$\Delta\Psi_{half} = \Psi^\pm - \Psi^{bulk} - \text{PZC}$) obtained in two ILs at both electrodes.